OBC
www.rsc.org/obc

$^{15}NH_4^+$ ion movement inside $d(G_4T_4G_4)_2$ G-quadruplex is accelerated in the presence of smaller Na^+ ions

Primož Šket,[a] Martin Črnugelj,[a] Wiktor Koźmiński[b] and Janez Plavec*[a]

[a] *NMR center, National Institute of Chemistry, Hajdrihova 19, SI-1000 Ljubljana, Slovenia. E-mail: janez.plavec@ki.si; Fax: +386 1 47 60 300; Tel: +386 1 47 60 353*

[b] *Department of Chemistry, University of Warsaw, u1. Pasteura 1, 02-093 Warsaw, Poland*

Received 6th May 2004, Accepted 1st June 2004
First published as an Advance Article on the web 16th June 2004

2D NMR studies demonstrate that the residence lifetime of $^{15}NH_4^+$ ions within the bimolecular G-quadruplex adopted by $d(G_4T_4G_4)$ is reduced from 270 ms in the presence of ammonium ions alone to 36 ms in the presence of Na^+ ions.

It is generally appreciated that cations play a central role in governing the structure, stability, dynamics and function of nucleic acids.[1,2] G-rich DNA oligonucleotides, for example, require the presence of monovalent cations to fold into G-quadruplexes, which are unique among nucleic acid structures in their sequence dependence and metal ion requirements.[3–20] The basic building block of a four-stranded G-quadruplex structure is a G-quartet with the four closely spaced carbonyl groups that are responsible for the strong cation coordination (Fig. 1a). The first high resolution structure of the G-quadruplex adopted by the sequence $d(G_4T_4G_4)$ was determined by both NMR[12] and X-ray crystallography.[21] This sequence forms a dimeric G-quadruplex, where four GGGG segments are involved in the formation of four stacked G-quartets with *syn–anti–anti–syn* orientations around each quartet, while both TTTT loops span across the diagonals of the outer quartets such that adjacent strands are in antiparallel and parallel orientations (Fig. 1b). The critical role that monovalent cations play in G-quadruplex formation initiated considerable efforts for identifying cation binding sites using NMR,[22–25] X-ray[21,26,27] and computational[28–30] techniques. In particular, molecular dynamics simulations on the nanosecond time-scale offered some insight into the cation mobility at the atomic level.[28–30] Two-dimensional ^1H–^{15}N NMR spectroscopy allowed direct location of three $^{15}NH_4^+$ ions, which were successfully used as a nonmetallic substitute for monovalent cations, between the adjacent G-quartets (Fig. 1b).[22] This approach also enabled analyses of $^{15}NH_4^+$ ion movement between the binding sites within the $d(G_4T_4G_4)_2$ G-quadruplex.[22] In contrast, X-ray structures revealed a linear ion array consisting of three potassium ions embedded between the planes of the G-quartets and two additional ions between the outer G-quartets and thymine loop residues of the $d(G_4T_4G_4)_2$ G-quadruplex.[21] Na^+ ions exhibit a smaller ionic radius that allows them to be coordinated in the plane of the G-quartet.[26,27] Li^+ ions are not known to stabilize G-quartet formation but are involved in the neutralization of negative charges along the sugar–phosphate backbone.[31,32]

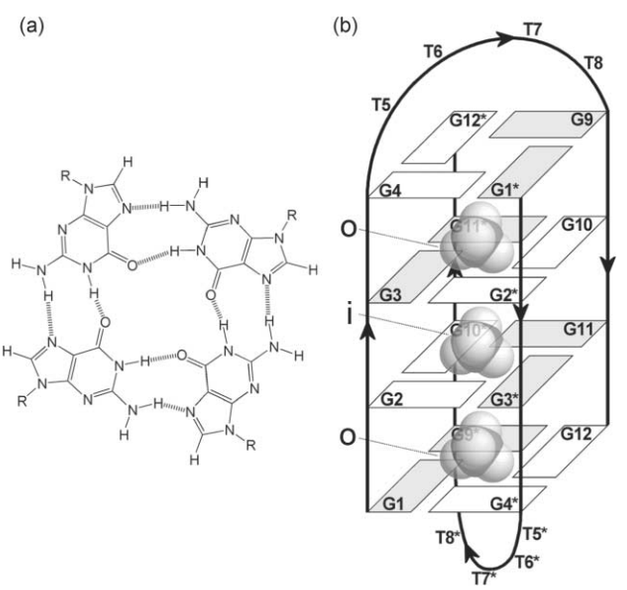

Fig. 1 a) The main feature of G-quartets are cyclic hydrogen bonds between four guanine bases in a coplanar arrangement. b) Location of ammonium ions in dimeric foldback structure adopted by $d(G_4T_4G_4)_2$. Labels **o** and **i** indicate ammonium ions at the outer and the inner binding sites, respectively. G1–G12 indicate nucleotide residues of one strand of $d(G_4T_4G_4)_2$, whereas G1*–G12* indicate residues of the symmetry related strand. The guanine bases are shown as rectangles, where filled grey rectangles represent *syn* nucleobases. For clarity, thymine bases are not shown.

In this work we have focused on $d(G_4T_4G_4)$ which has been shown to form a G-quadruplex with the same general fold in the presence of $^{15}NH_4^+$, K^+ and Na^+ ions.[14] A recent study of $^{15}NH_4^+$ ion exchange within the $d(G_4T_4G_4)_2$ G-quadruplex afforded an estimate of 250 ms for the lifetime of the inner ammonium ion at 283 K.[22] On the other hand, ^{23}Na NMR linewidth studies with the same G-quadruplex revealed the lifetime of bound Na^+ to be 180 μs at 293 K.[33] The significant difference in the lifetime values for $^{15}NH_4^+$ and Na^+ ions inspired us to explore if the movement of $^{15}NH_4^+$ ion changes with an increase of ionic strength or when smaller Na^+ ions partially occupy binding sites inside $d(G_4T_4G_4)_2$. We herein report our initial results on acceleration of $^{15}NH_4^+$ ion movement by *ca.* 7.5-times from the inner to the outer binding sites of $d(G_4T_4G_4)_2$ as Na^+ ion occupancy of the binding sites progressively increases with the increase in the $NaCl/^{15}NH_4Cl$ ratio.

$d(G_4T_4G_4)$ was folded into a G-quadruplex structure upon titration of $^{15}NH_4Cl$ into aqueous solution that was extensively dialyzed against 10 mM LiCl in order to remove all other cations.† Titration of $^{15}NH_4Cl$ into one part of the oligonucleotide sample up to a 20 mM concentration resulted in well resolved imino, aromatic and sugar proton resonances in the ^1H NMR spectrum at 600 MHz, which were consistent with the known solution-state fold-back structure of $d(G_4T_4G_4)_2$.[12] Analysis of the 2D ^{15}N–^1H NzExHSQC spectrum shown in Fig. 2 revealed three autocorrelation peaks corresponding to $^{15}NH_4^+$ ions in the bound states, occupying the outer (**o**) and the inner (**i**) binding sites, as well as ions in bulk solution (**b**).[22] No specific $^{15}NH_4^+$ ion binding sites between the outer G-quartets and residues of the T_4 loops were observed. Further NMR studies including detailed NOESY analysis for $d(G_4T_4G_4)_2$ also showed no specific NOE cross-peaks for the potential ion binding sites in the T_4 loops of $d(G_4T_4G_4)_2$.[14] Experimental data,

DOI: 10.1039/b406815g

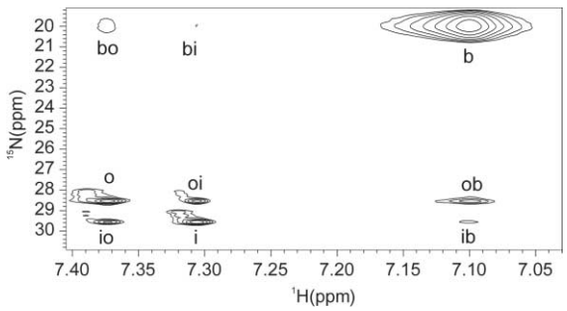

Fig. 2 Plot of 2D ^{15}N–^{1}H NzExHSQC spectrum (τ_m = 100 ms) of $^{15}NH_4^+$ form of d($G_4T_4G_4$)$_2$ G-quadruplex at 298 K. The autocorrelation peaks for the two bound sites are labeled (**i** for the inner and **o** for the outer sites) and for bulk (**b**) ammonium ions. Cross-peaks indicate $^{15}NH_4^+$ ion movement between these three sites (see text).

however, do not exclude the existence of ion exchange with bulk solution that is fast on the NMR time-scale.‡ Several cross-peaks (labeled as **oi**, **io**, **ob**, **ib**, **bo** and **bi**) in addition to three autocorrelation peaks were identified in the 2D ^{15}N–^{1}H NzExHSQC spectrum and clearly indicated that $^{15}NH_4^+$ ions moved from one binding site to another. In particular, the cross-peak labeled **io** demonstrated that some $^{15}NH_4^+$ ions moved from the inner to the outer binding sites during the mixing time (Figs. 1b and 2).

The **io** cross-peaks are characterized by the ^{15}N chemical shift of ammonium ions at the inner binding site (δ_{15N} = 29.5 ppm) that moved during the mixing time and have been detected at the ^{1}H chemical shift of the outer binding sites (δ_{1H} = 7.372 ppm). Time evolution of exchange of ammonium ions from the inner to the outer binding sites can be appreciated by comparison of the traces at the ^{15}N chemical shift of 29.5 ppm through **i** and **io** cross-peaks in the 2D spectrum (Fig. 3a). Signal intensity of **i** decreases, while intensity of **io** increases with increasing mixing time. The relative integral ratio of **io** *versus* **i** signals is *ca.* 0.3 at a mixing time of 100 ms and increases to 0.7 at a mixing time of 450 ms. Analysis of the time-dependence of autocorrelation and cross-peak intensities as a function of mixing time showed that signal decrease due to (T_1) relaxation is not significant at mixing times up to 200 ms.

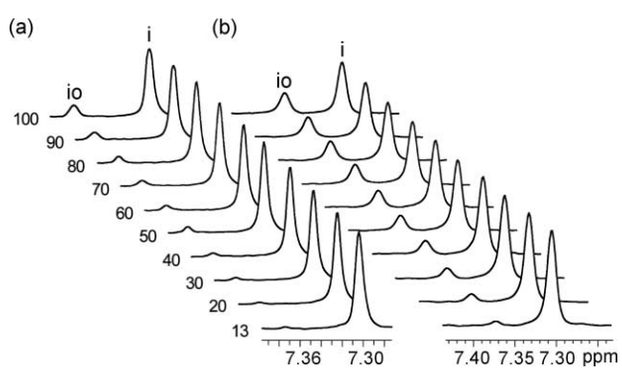

Fig. 3 Traces along f2 dimension of 2D ^{15}N–^{1}H NzExHSQC spectrum at δ_{15N} of 29.5 ppm as a function of increasing mixing time given in ms on the left. a) d($G_4T_4G_4$)$_2$ sample folded in the presence of 20 mM $^{15}NH_4Cl$; b) the same G-quadruplex in the presence of 20 mM $^{15}NH_4Cl$ and 5 mM NaCl.

d($G_4T_4G_4$) was also folded into the G-quadruplex structure in the presence of 20 mM $^{15}NH_4Cl$ and 5 mM NaCl.† A detailed comparative examination of 1D and 2D ^{1}H NMR spectra of d($G_4T_4G_4$)$_2$ in the presence of $^{15}NH_4Cl$ alone and in the presence of both $^{15}NH_4Cl$ and NaCl showed the highest degree of agreement, which led us to the reasonable conclusion that their 3D structures are identical. Furthermore, 2D ^{15}N–^{1}H NzExHSQC spectra for d($G_4T_4G_4$)$_2$ quadruplex folded in the presence of both $^{15}NH_4^+$ and Na^+ ions showed autocorrelation and cross-peaks at the identical ^{15}N and ^{1}H chemical shifts as found for $^{15}NH_4^+$ ion only form (Fig. 2). The comparison of intensities of **o** and **i** cross-peaks in the spectra of the two samples, however, showed a reduction of approximately 18% and 15%, respectively, which suggested that the outer and the inner binding sites were partially occupied by sodium ions in the 20 mM $^{15}NH_4^+$ and 5 mM Na^+ sample. It was particularly exciting to observe that the cross-peak intensities exhibited distinctive changes as a function of mixing time in the presence of both ions and $^{15}NH_4^+$ ions alone. Time evolution of ammonium ion movement from the inner to the outer binding sites in the presence of 20 mM $^{15}NH_4Cl$ and 5 mM NaCl is illustrated by the comparison of traces at ^{15}N chemical shift of 29.5 ppm through **i** and **io** cross-peaks in the 2D spectra (Fig. 3b). The comparison of Figs. 3a and b shows that **io** intensity increases faster in the mixed ammonium–sodium sample. The **io/i** ratio in the sample containing 20 mM $^{15}NH_4Cl$ and 5 mM NaCl was 0.5 at a mixing time of 100 ms, whereas it was 0.3 in the ammonium only form. The **io** signal reaches maximum intensity at shorter mixing times (100 ms) in the presence of Na^+ ions in comparison to the ammonium only sample (200 ms).

Quantification of volume integrals of the **io** cross-peak with respect to its autocorrelation peak **i** as a function of increasing mixing time in the presence of $^{15}NH_4^+$ ions alone (Fig. 4) was then used to calculate the exchange rate of ammonium ion movement from the inner to the outer binding sites. The time-dependence of the ratio of the **io** cross-peak and its autocorrelation peak volumes at shorter mixing times can be expressed by eqn. 1,[34]

$$\frac{V_{io}}{V_i} = \tanh\left(k_{io}^{a}\tau_m\right) \qquad (1)$$

where V_{io} and V_i represent volume integrals of **io** and **i** peaks, respectively, tanh is a hyperbolic tangent function, k_{io}^{a} is the rate constant for $^{15}NH_4^+$ ion movement from the inner to the outer binding sites in d($G_4T_4G_4$)$_2$ G-quadruplex in the presence of ammonium ions alone, and τ_m is the mixing time of the 2D ^{15}N–^{1}H NzExHSQC experiment. The least-squares fit of the experimental ratio of V_{io}/V_i as a function of mixing time gave a rate constant k_{io}^{a} of 3.7 s^{-1} for d($G_4T_4G_4$)$_2$ in 20 mM $^{15}NH_4Cl$ (Fig. 4). The agreement between the experimental and calculated data points was excellent, with individual deviations below 0.01 unit and chi-squared of 0.00008 (Person correlation coefficient, R = 0.997). The lifetime for the ammonium ion occupying the inner binding site of the d($G_4T_4G_4$)$_2$ at 20 mM $^{15}NH_4Cl$ is thus 270 ms, which correlates well with previously published data.[22] An analogous iterative fit of the experimental

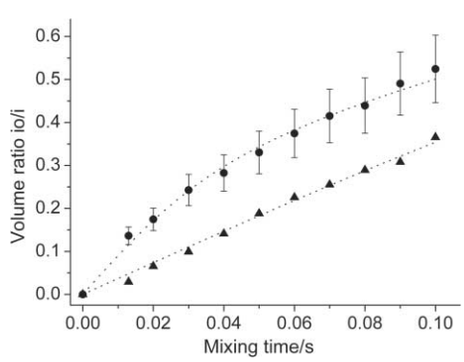

Fig. 4 Volume ratios of **io** cross-peak and its autocorrelation peak **i** as a function of mixing time at 298 K. Triangles represent the experimental points for sample with $^{15}NH_4^+$ ions alone (*i.e.* 20 mM $^{15}NH_4Cl$). Circles correspond to experimental points for 20 mM $^{15}NH_4Cl$ and 5 mM NaCl sample. Vertical bars indicate scattering of experimental points at different concentration ratios of $^{15}NH_4^+$ and Na^+ ions. Dotted curves represent the best fit of the experimental data to eqns. 1 and 2.

Table 1 Ammonium ion exchange rates in $d(G_4T_4G_4)_2$ G-quadruplex[a]

#[b]	$[^{15}NH_4^+]$/mM	$[Na^+]$/mM	$[Na^+]/[^{15}NH_4^+]$	k_{io}/s^{-1}	f_a (%)	individual deviation/s^{-1}	chi-squared	% Na at **o**[d]	% Na at **i**[d]
1	20	0	0	3.7	100	0.01	0.00008	0	0
2	40	5	0.125	24	66	0.02	0.00027	16	14
3	20	5	0.25	27	77	0.02	0.00028	18	15
4	40	25	0.625	33	73	0.03	0.00040	39	33
5	20	15	0.75	25	78	0.02	0.00024	35	30
6	40	35	0.875	30	72	0.02	0.00029	46	41
7	20	25	1.25	33	78	0.03	0.00030	55	50
8	20	35	1.75	42	82	0.04	0.00037	79	74
9	8	20	2.5	—	89[c]	0.10	0.00200	93	94

[a] At 2.4 mM concentration per strand, 298 K and pH of 5.0. [b] Error estimates in rate constants are ±0.1 s^{-1} for ammonium only form (#1) and ±4 s^{-1} for mixed ammonium–sodium forms. Largest individual deviation and chi-squared values are reported for each iterative fitting procedures using eqns. 1 and 2. [c] Calculated using eqn. 2 by constraining k_{io}^{m} rate constant to average value of 28 s^{-1}. [d] Partial occupancy (in %) of the outer and the inner binding sites by sodium ions.

ratio of V_{io}/V_i for the $d(G_4T_4G_4)_2$ sample in the presence of 20 mM $^{15}NH_4^+$ and 5 mM Na^+ ions using eqn. 1 did not fit the data (individual deviations > 0.06 units, chi-squared = 0.0015, R = 0.970). In particular, the shape of the function through the experimental data points suggested a contribution of an additional faster processes to the observed rate in the sample containing both $^{15}NH_4^+$ and Na^+ ions, which prompted us to include two processes in further analysis. Ammonium ion movement from the inner to the outer binding sites, which are occupied by ammonium ions or partially by sodium ions in the mixed ammonium–sodium form can be described by the following simplified scheme:

$$\text{inner}^{a} \xrightarrow{k_{io}^{a}} \left[\text{outer}^{a} + \text{outer}^{m}\right] \xleftarrow{k_{io}^{m}} \text{inner}^{m}$$

Parameters k_{io}^{a} and k_{io}^{m} are exchange rate constants, which correspond to the movement of $^{15}NH_4^+$ ions from the inner to the outer positions in the ammonium only and in a mixed ammonium–sodium form, respectively. Both exchange steps in the above scheme, which proceed independently of each other in two different molecules, give rise to a single **io** cross-peak in the 2D ^{15}N–^{1}H NzExHSQC spectrum with isochronous ^{1}H and ^{15}N chemical shifts (Fig. 2). The experimentally observed time-dependence of **io** cross-peak intensity contains contributions from $^{15}NH_4^+$ ion exchange in both forms and therefore represents a weighted time-average of exchange on the NMR time-scale. The ratio of volume integrals of **io** cross-peak and **i** autocorrelation peak as a function of mixing time can thus be expressed by eqn. 2,

$$\frac{V_{io}}{V_i} = f_a \tanh\left(k_{io}^{a}\tau_m\right) + \left(1 - f_a\right)\tanh\left(k_{io}^{m}\tau_m\right) \qquad (2)$$

where f_a represents a fraction of the exchange process in ammonium only form. The assumption made in the first term of eqn. 2 is that the k_{io}^{a} exchange rate constant in ammonium only G-quadruplex is not affected by the presence of Na^+ ions in bulk solution or by nearby mixed ammonium–sodium forms. The second term accounts for the dynamics of ammonium ion exchange inside G-quadruplex molecules where some of the binding sites are partially occupied by sodium ions. The least-squares fit through the experimental data points using eqn. 2 resulted in the k_{io}^{m} rate constant of 27 s^{-1}, which corresponds to a lifetime of 37 ms for $^{15}NH_4^+$ ions in the mixed ammonium–sodium forms (Fig. 4). The estimated contribution of the ammonium only form (f_a) to the experimentally observed **io/i** cross-peak ratio was 77%.

In further experiments we examined whether the experimentally determined ammonium ion exchange rate was sensitive to a change in the concentration and possibly relative ratios of $^{15}NH_4^+$ and Na^+ ions. The $d(G_4T_4G_4)_2$ G-quadruplex was formed in the presence of 20 and 40 mM $^{15}NH_4Cl$ together with 5, 15, 25 or 35 mM NaCl. Perusal of NMR spectra at various $^{15}NH_4^+/Na^+$ ratios showed full agreement with the data for the ammonium only solution when the concentration of Na^+ ions was below 25 mM. At 20 mM $^{15}NH_4Cl$ and 25 mM NaCl the ^{1}H NMR spectrum revealed the presence of small peaks corresponding to the minor (≤10%) sodium form of $d(G_4T_4G_4)_2$ with the majority of G-quadruplex in ammonium form but with some binding sites partially occupied by Na^+ ions. The further increase of NaCl concentration to 35 mM at the same concentration of $^{15}NH_4Cl$ resulted in 50% of the sodium form of $d(G_4T_4G_4)_2$ in solution. The ^{1}H NMR spectrum of the 20 mM NaCl and 8 mM $^{15}NH_4Cl$ sample showed protons of major (*ca.* 85%) sodium form of $d(G_4T_4G_4)_2$ and smaller peaks corresponding to 15% of mixed ammonium–sodium forms of the same G-quadruplex.

A series of NzExHSQC experiments with mixing times in the range from 13 ms to 225 ms were acquired for the $d(G_4T_4G_4)_2$ at different concentrations of $^{15}NH_4^+$ and Na^+ ions and were used to calculate k_{io}^{m} rate constants and f_a values using eqn. 2 (Table 1). Increases in $^{15}NH_4^+$ concentration from 20 mM to 40 mM, while maintaining the 5 mM Na^+ ion concentration, resulted in a minor change for the k_{io}^{m} rate constant that is within the error limits of the experiment. The fraction that the ammonium only form contributed to the overall exchange rate dropped from 77% to 66% (entries 3 and 2 in Table 1). The k_{io}^{m} rate constants for samples with Na^+ ion concentrations increasing from 5 to 25 mM were within the range from 24 s^{-1} to 33 s^{-1} at both 20 mM and 40 mM $^{15}NH_4^+$, whereas f_a values varied from 66% to 78%. All of the least-squares fits exhibited satisfactory agreement with experimental data (Table 1). Integration of autocorrelation and cross-peaks for 20 mM $^{15}NH_4^+$ and 35 mM Na^+ ion sample was less accurate due to their weaker intensities in the 50% presence of the sodium only form of $d(G_4T_4G_4)_2$ in solution and resulted in a k_{io}^{m} rate constant of 42 s^{-1} which contributed 18% to the overall exchange rate (entry 8 in Table 1). The uncertainty in integration of weak **io** and **i** cross-peaks was even more pronounced for the 8 mM $^{15}NH_4^+$ and 20 mM Na^+ ion sample and precluded quantitative analysis in the analogous way.

Individual k_{io}^{m} rate constants were used to calculate an average value of 28 s^{-1} with a standard deviation of 4 s^{-1} (entries 8 and 9 were not included in the calculation). It is noteworthy that different ratios of $^{15}NH_4Cl$ and NaCl resulted in almost the same rate constant for the **io** cross-peak with standard deviation that was comparable to the error of the measurements. The average contribution of the ammonium only form to the observed rate constant (f_a) was 74% (std. deviation = 4%). No correlation between the fractions that

the ammonium form contributed to the overall exchange rate and $^{15}NH_4^+/Na^+$ concentration ratios could be established.

The accuracy of the k_{io}^m rate constant was intrinsically hampered by the fact that only *ca.* 26% of the experimentally observed exchange was due to ammonium ion movement in the mixed ammonium–sodium forms of the G-quadruplex. In further analysis we made use of the average k_{io}^m rate constant and calculated fractions (f_a') that inner $^{15}NH_4^+$ ions contribute to the overall exchange rates at several $^{15}NH_4^+$ and Na^+ concentrations. The results of iterative fitting using eqn. 2 where k_{io}^m was constrained to 28 s^{-1} gave satisfactory agreements with experimental data and showed the following: (i) f_a' values were very close to f_a values with the biggest difference being 3 unit%, and (ii) f_a' values were found in the range between 68 and 79% with the average f_a' value of 74% (std. deviation = 4%) which is identical to the average f_a value.

The k_{io}^m rate constants were obtained at several $^{15}NH_4^+/Na^+$ ratios. A Na^+ ions addition as small as 5 mM resulted in the increase of $^{15}NH_4^+$ ion movement from the inner to the outer binding sites in the mixed ammonium–sodium forms to the maximum value of 28 s^{-1}. The addition of Na^+ ions results in partial occupancy of some of the binding sites, which accelerates $^{15}NH_4^+$ ion movement, whereas ion concentration in bulk solution does not exert noticeable influence on the $^{15}NH_4^+$ ion movement from the inner to the outer binding sites inside of the G-quadruplex. Along these lines, the k_{io}^m rate constant at the smallest amount of Na^+ ions already corresponds to $^{15}NH_4^+$ movement from the inner binding site to replace Na^+ ion at the outer binding site of mono-sodium/di-ammonium form of $d(G_4T_4G_4)_2$ G-quadruplex. Further increase in the concentration of such mono-sodium species or even appearance of di-sodium form apparently does not lead to further increase in the rate of $^{15}NH_4^+$ ion movement. At this stage experimental determination of the $Na^+/^{15}NH_4^+$ ratio that already leads to di-sodium/mono-ammonium structures of G-quadruplex is elusive. Nevertheless, the k_{io}^m rate constant represents a good estimate for $^{15}NH_4^+$ ion movement from the inner to the outer binding sites where Na^+ ion movement is not rate limiting. This movement is considerably slower when all binding sites are completely occupied by ammonium ions which requires partial opening of individual G-quartets for the $^{15}NH_4^+$ ions to move through the central ion cavity of the G-quadruplex (*i.e.* double $^{15}NH_4^+$ movement).

In summary, NMR study of ammonium ion movement inside $d(G_4T_4G_4)_2$ G-quadruplex reported here shows that dynamics of ammonium ions is influenced by smaller sodium ions. The lifetime of the inner $^{15}NH_4^+$ ion at 298 K is 270 ms when only ammonium ions are present in solution. The lifetime for the inner $^{15}NH_4^+$ ions in the mixed ammonium–sodium forms is 36 ms. Further increase in the concentration of NaCl in solution leads to higher Na^+ ion occupancy of the binding sites but does not increase the exchange rate of inner $^{15}NH_4^+$ ions. We feel that the present findings represent a significant step toward understanding the complexity of exchange and dynamics of ions inside G-quadruplex structures and nucleic acids in general.

Acknowledgements

We thank the Ministry of Education, Science and Sport of the Republic of Slovenia (Grant No. J1-3309-0104 and P1-0242-0104) and European Commission (Contract No. ICA1-CT-2000-70034) for their financial support.

Notes and references

† DNA oligonucleotide $d(G_4T_4G_4)$ (Oxy-1.5) was synthesized on an Expedite 8909 synthesizer using phosphoramidite chemistry following the manufacturer's protocol. DNA was purified on a 1.0 m Sephadex G15 column. Fractions containing only full-length oligonucleotide were pooled, lyophilized, redissolved in 1 ml of H_2O and dialyzed extensively against 10 mM LiCl solution. The concentration of Na^+ ions in the dialysed sample was well below 0.5 mM. The same sample was split into several equivalent portions with a concentration of 2.4 mM in strand (1.2 mM in G-quadruplex). TMSPA was used as reference. HCl was added to adjust the pH of the samples to 5.0. $^{15}NH_4Cl$ was titrated into the samples to a total 20 or 40 mM concentration for each sample. NaCl was titrated to 5, 15, 25 and 35 mM concentration.
‡ All NMR spectra were collected on a Varian Unity Inova 600 MHz NMR spectrometer at 298 K. The 2D ^{15}N–^1H NzExHSQC spectra were acquired with 832 complex points in F2 and 128 increments in F1 dimensions, eight scans for each increment, and a spectral width of 4000 Hz in F2 and 1000 Hz in F1 dimensions. NzExHSQC spectra were acquired at mixing times of 13, 20, 30, 40, 50, 60, 70, 80, 90, 100, 120, 140, 160, 180, 200 and 225 ms (including the inherent 13 ms delay). The additional longer mixing times of 250, 275, 300, 350, 400, 450, 600, 800, 1000, 1200, 1500 and 2000 ms were also acquired for sample containing 20 mM $^{15}NH_4Cl$. Standard HSQC experiment was used to determine $^{15}NH_4^+/Na^+$ ion occupancy of the binding sites. ^{23}Na 1D spectra were collected on a Varian Unity plus 300 MHz NMR spectrometer using a standard one-pulse sequence.

1 N. V. Hud and M. Polak, *Curr. Opin. Struct. Biol.*, 2001, **11**, 293–301.
2 N. V. Hud and J. Plavec, *Biopolymers*, 2003, **69**, 144–159.
3 M. A. Keniry, *Biopolymers*, 2001, **56**, 123–146.
4 C. C. Hardin, A. G. Perry and K. White, *Biopolymers*, 2001, **56**, 147–194.
5 R. H. Shafer and I. Smirnov, *Biopolymers*, 2001, **56**, 209–227.
6 S. Neidle and M. A. Read, *Biopolymers*, 2001, **56**, 195–208.
7 J. T. Davis, *Angew. Chem., Int. Ed.*, 2004, **43**, 668–698.
8 G. D. Strahan, R. H. Shafer and M. A. Keniry, *Nucleic Acids Res.*, 1994, **22**, 5447–5455.
9 F. W. Smith, F. W. Lau and J. Feigon, *Proc. Natl. Acad. Sci. USA*, 1994, **91**, 10546–10550.
10 M. Crnugelj, N. V. Hud and J. Plavec, *J. Mol. Biol.*, 2002, **320**, 911–924.
11 M. Crnugelj, P. Sket and J. Plavec, *J. Am. Chem. Soc.*, 2003, **125**, 7866–7871.
12 F. W. Smith and J. Feigon, *Nature*, 1992, **356**, 164–168.
13 N. V. Hud, F. W. Smith, F. A. L. Anet and J. Feigon, *Biochemistry*, 1996, **35**, 15383–15390.
14 P. Schultze, N. V. Hud, F. W. Smith and J. Feigon, *Nucleic Acids Res.*, 1999, **27**, 3018–3028.
15 A. Kettani, S. Bouaziz, A. Gorin, H. Zhao, R. A. Jones and D. J. Patel, *J. Mol. Biol.*, 1998, **282**, 619–636.
16 D. Miyoshi, A. Nakao, T. Toda and N. Sugimoto, *FEBS Lett.*, 2001, **496**, 128–133.
17 G. N. Parkinson, M. P. H. Lee and S. Neidle, *Nature*, 2002, **417**, 876–880.
18 M. S. Searle, H. E. L. Williams, C. T. Gallagher, R. J. Grant and M. F. G. Stevens, *Org. Biomol. Chem.*, 2004, **2**, 810–812.
19 A. T. Phan and D. J. Patel, *J. Am. Chem. Soc.*, 2003, **125**, 15021–15027.
20 D. Gomez, T. Lemarteleur, L. Lacroix, P. Mailliet, J. L. Mergny and J. F. Riou, *Nucleic Acids Res.*, 2004, **32**, 371–379.
21 S. Haider, G. N. Parkinson and S. Neidle, *J. Mol. Biol.*, 2002, **320**, 189–200.
22 N. V. Hud, P. Schultze, V. Sklenar and J. Feigon, *J. Mol. Biol.*, 1999, **285**, 233–243.
23 D. Rovnyak, M. Baldus, G. Wu, N. V. Hud, J. Feigon and R. G. Griffin, *J. Am. Chem. Soc.*, 2000, **122**, 11423–11429.
24 G. Wu and A. Wong, *Chem. Commun.*, 2001, 2658–2659.
25 G. Wu, A. Wong, Z. H. Gan and J. T. Davis, *J. Am. Chem. Soc.*, 2003, **125**, 7182–7183.
26 K. Phillips, Z. Dauter, A. I. H. Murchie, D. M. J. Lilley and B. Luisi, *J. Mol. Biol.*, 1997, **273**, 171–182.
27 M. P. Horvath and S. C. Schultz, *J. Mol. Biol.*, 2001, **310**, 367–377.
28 N. Spackova, I. Berger and J. Sponer, *J. Am. Chem. Soc.*, 1999, **121**, 5519–5534.
29 N. Spackova, I. Berger and J. Sponer, *J. Am. Chem. Soc.*, 2001, **123**, 3295–3307.
30 S. Chowdhury and M. Bansal, *J. Phys. Chem. B*, 2001, **105**, 7572–7578.
31 O. L. Acevedo, L. A. Dickinson, T. J. Macke and C. A. Thomas, *Nucleic Acids Res.*, 1991, **19**, 3409–3419.
32 J. F. Chantot and W. Guschlbauer, *FEBS Lett.*, 1969, **4**, 173–176.
33 H. Deng and W. H. Braunlin, *J. Mol. Biol.*, 1996, **255**, 476–483.
34 M. H. Levitt, *Spin Dynamics: Basics of Nuclear Magnetic Resonance*, John Wiley & Sons, Ltd, Chichester, 2001.